Remote Sensing of Environment 264 (2021) 112584

Contents lists available at ScienceDirect

Remote Sensing of Environment

journal homepage: www.elsevier.com/locate/rse

How to automate timely large-scale mangrove mapping with remote sensing

Ying Lu, Le Wang *

Department of Geography, University at Buffalo, The State University of New York, 105 Wilkson Quad, Buffalo, NY 14261, USA

ARTICLE INFO

Editor: Marie Weiss

Keywords:
Large-scale mapping
Mangrove forests
Training sample collection
One-class classification
Region growing
Remote sensing
Landsat
Sentinel
Google Earth Engine

ABSTRACT

Mangrove forests have witnessed significant changes resulted from both anthropogenic and natural disturbances in the last four decades. Although a few attempts have been reported, effective methods that can repeatedly generate large-scale mangrove maps on a timely basis are still lacking due to the difficulty in gathering sufficient training samples in large geographical areas. In this study, we have addressed three objectives in the following manner: (1) we aim to develop a method to automatically collect ample mangrove training samples; Correspondingly, we developed an automatic training sample collection method which extracted unchanged mangrove samples from a historical mangrove map; In addition, we employed a region growing method to include more diversified training samples; (2) we strive to foster compatible classifiers that can leverage the collected one-class training samples; To this end, we came up with two representative one-class classifiers: the Support Vector Data Description (SVDD), and the Positive and Unlabeled Learning algorithm (PUL); (3) we endeavor to compare the effectiveness of various combinations of training samples, classifiers, and input images; As a result, we developed 32 classification models by varying four different variables: training samples (unchanged vs. expanded), input data (Landsat 8, Sentinel-1, and Sentinel-2), classifiers (SVDD vs. PUL), and study sites (Florida, the United States and Guangxi, China). We found that our developed automatic training sample collection methods performed well (user's accuracy >97%). Inter-annual NDVI combined with geometric restrictions warranted the effective extraction of unchanged training samples while the region growing method further reduced the omission due to its addition of recently emerged mangroves. In addition, PUL performed better than SVDD. This is attributed to the fact that PUL draws upon not only mangrove samples, but also unlabeled ones unaccounted for in SVDD. Lastly, the combination of Sentinel-1 and Sentinel-2 is recommended among all the compared models. In summary, we developed an effective method to automatically extract mangrove training samples, based on which a one-class classification method for large-scale mangrove mapping is made possible. We envision our methods will contribute to a wide spectrum of timely large-scale mangrove mapping tasks.

1. Introduction

Mangrove forests are shrubs or trees distributed along coastal areas between approximately 30° N and 30° S latitude (FAO, 2007; Giri et al., 2011). They are treated as a cradle of biological diversity due to their excellent capability of decontamination, water conservation and nutrient storage (Kathiresan, 2003; Mumby et al., 2004). Thanks to their heavy root systems which conserve massive carbon and nutrients, the organic carbon fixation capacity of mangrove forests is almost four times greater than that of other terrestrial forests, making mangrove forests indispensable for global carbon cycle studies (Donato et al., 2011). Moreover, due to the rich food webs and stable environment, mangrove forests are excellent food obtaining sites and perfect shelters. For example, they support various organisms from bacteria to large predators both in the forests and offshore areas (Blaber and Milton, 1990). Therefore, mangrove forests play a significant role for studies on the global carbon cycle and biodiversity (Wang et al., 2019).

Nevertheless, for the last four decades, mangrove forests have been continuously shrinking as a result of human activities and climate change (Nicholls and Cazenave, 2010; Richards and Friess, 2016). About 35% of mangrove forests have disappeared from the year 1980 to 2000 worldwide (Schaffelke et al., 2005; Valiela et al., 2001). The global deforestation rate in mangrove biomes from 2000 to 2012 was 4.73%, with an annual loss rate of 0.39% (Hamilton and Casey, 2016). The

* Corresponding author.
E-mail addresses: ylu26@buffalo.edu (Y. Lu), lewang@buffalo.edu (L. Wang).

https://doi.org/10.1016/j.rse.2021.112584
Received 19 January 2021; Received in revised form 28 June 2021; Accepted 2 July 2021
Available online 20 July 2021

primary cause for the shrinking is the conversion of mangrove forests to aquaculture (Alongi, 2009). About one third of the coastal and offshore adult fish caught in Southeast Asia develop in mangrove forests (Alongi, 2009). Such a rapid change compounded by various deforestation activities have led to an urgent demand for mapping mangrove distributions at a large scale on a timely basis.

To our knowledge, since 2010, large-scale mangrove mapping has become more and more automatic to satisfy the requirement of timely mapping (Chen et al., 2017; Giri et al., 2015; Giri et al., 2011; Jia et al., 2014a; Thomas et al., 2017; Tieng et al., 2019). Before 2010, large-scale mangrove products were compilations of local or national mangrove maps (FAO, 2007; Spalding et al., 2010). They were not consistent and not comparable in different locations. In order to solve this problem, Giri et al. (2011) generated the first comprehensive, globally consistent and high-resolution mangrove map, the Mangrove Forests of the World database (MFW), using hybrid supervised and unsupervised digital image classification techniques. This map offered a good reference for global forests and carbon cycle studies. It was widely acknowledged as a reference in a large part of national or global forests studies (Hamilton and Casey, 2016; Thomas et al., 2018). However, in the process of unsupervised classification, they had to interpret and label mangrove areas in approximately 1000 Landsat scenes globally, according to field data and high-resolution imagery scene-by-scene. Timely repeating their method to produce new mangrove maps was difficult. Thus, in recent years, many studies have been proposed to address this problem by promoting the automation of mangrove mapping methods (Bunting et al., 2018; Hamilton and Casey, 2016; Thomas et al., 2018; Yancho et al., 2020). Instead of using remote sensing imagery, Hamilton and Casey (2016) mapped global mangrove cover annually at high spatial resolution using existing forest and terrestrial ecosystem products. Using MFW from the year 2000 as a baseline, the Global Forest Change database (GFC) (Hansen and DeFries, 2004) was queried for deforestation to produce a new mangrove map for the year 2001. This process was repeated for every year from 2001 to 2012. In addition, forest changes in the entire mangrove biome were mapped by integrating the Terrestrial Ecosystem of the World database (Olson et al., 2001) and GFC using the same method. Finally, they successfully mapped the sub-pixel mangrove fractions, and detected the deforestation patterns of global mangrove forests and mangrove biome from 2000 to 2012. Nevertheless, their method relied on existing map products, which may cause error accumulation. The updating period of this map had to follow the update of these products. Moreover, newly planted mangrove forests were not able to be delineated in their mangrove maps. To avoid these issues, supervised mangrove mapping methods using remote sensing imagery are widely utilized (Bunting et al., 2018; Chen et al., 2017; Yancho et al., 2020). Among these efforts, one of the most compelling studies was proposed by Bunting et al. (2018). It was the first time a new global mangrove forest distribution database, the Global Mangrove Watch (GMW), was created with a globally consistent and automated classification method. In lieu of unsupervised classifiers, they developed a two-iteration mangrove mapping method with a supervised classifier, the Extremely Randomized Trees classifier. Advanced Land Observing Satellite data and Landsat imagery, which are complementary to each other, were used as data sources. Nevertheless, in order to ensure the high accuracy of mangrove mapping, visual interpretation was applied in most processes: In the creation of a mangrove habitat mask, the results should be checked manually one by one; For the classification of mangrove and non-mangrove land covers, visual interpretation was required to check and edit the training data. It may cost several weeks even with well-trained staff. In addition, Yancho et al. (2020) developed a new tool, the Google Earth Engine Mangrove Mapping Methodology, to monitor the extent of mangrove forests worldwide. It is a tool that can be easily accessed and reused by "non-specialist coastal managers and decision makers." In addition, this tool has a proven ability to successfully map mangrove forests in Myanmar. Overall accuracies for both historical and contemporary mangrove maps they made were all above 97%. Thus, it has a high potential for application in large-scale mangrove mapping. However, training samples in this study were still manually collected. Therefore, to further expedite the automation, three contingent questions must be addressed: How to timely collect ample training samples for large-scale mangrove mapping? Which supervised classification method is suitable for these training samples? Which combination of training samples, classifiers, and input images are better for large-scale mangrove mapping?

Training samples have a hard time to be updated as they were traditionally collected from fieldwork, published literature, training sample products, or visual interpretation (Friedl et al., 2002; Mahdianpari et al., 2020; Tian et al., 2020). In order to ease the way in training sample collection, existing historical maps were used as a reference in many large-scale mapping studies (Chen et al., 2016; Radoux et al., 2014; Thomas et al., 2018). However, since the distribution of land covers is changing with time and most mangrove map products are not 100% accurate, historical maps cannot represent current land cover distribution. Simple processing procedures, such as calculating intersections of different historical maps or making a possibility map for each land cover, are not enough. A great number of mislabeled pixels still exist. In order to collect high-quality training samples, visual interpretation or further processing are required. Fortunately, an automatic training sample collection method in large-scale land cover mapping offers encouragement. Radoux et al. (2014) believed that pixels along geographical boundaries between two different land cover types were more likely to be incorrectly labeled. In addition, they assumed that for each land cover type, spectral signatures were normally distributed. Thus, pixels along boundaries and pixels which were outliers in spectral signatures were all discarded to create a training sample dataset. However, for large-scale mangrove training sample collection, how to define the boundary of mangrove forests and how to find an index to remove outliers are still questioned.

Besides the challenge of training samples, a viable classification method is still required. The commonly used supervised classification methods for mangrove mapping are decision tree and maximum likelihood classifiers as they required relatively less amount of training samples when compared with other machine learning methods, such as deep learning (Diniz et al., 2019; Giri, 2016). However, they required training samples for all the land covers in mangrove ecoregions, which are still difficult to collect at large scales. By contrast, one-class classifiers only require samples for a target land cover, which saves time and labor in training sample collection (Khan and Madden, 2014). According to the training data they used, one-class classification can be classified into two categories. The first one only requires training samples for the target land cover (Khan and Madden, 2014; Tax and Duin, 1999a; Tax and Duin, 1999b). They aim to develop a boundary around the samples in feature space. Only objects inside the boundary are classified as the target land cover. Another category of one-class classification is trained with randomly collected unlabeled data and samples for the target land cover (Chen et al., 2016; Denis et al., 2002; Khan and Madden, 2014). The possibility of a pixel as the target land cover can be derived by comparing it to these two sample sets. However, to our knowledge, neither of the two categories of one-class classifiers have been used in large-scale mangrove mapping. Thus, it is worthwhile to exploit the performance of one-class classifiers in large-scale mangrove mapping.

To investigate automatic mangrove mapping methods, one inevitable question is what kinds of remote sensing data can be employed. Before Sentinel imagery became available, Landsat imagery was the primary data source for large-scale mangrove mapping because they are available globally and have full temporal coverage starting from 1972 (Giri et al., 2015; Islam, 2017; Long et al., 2014). In recent years, as Sentinel imagery offers Synthetic Aperture Radar (SAR) images unaffected by clouds and multi-temporal optical images with higher temporal and spatial resolution, a lot of researchers started to use them (Chen et al., 2017; Jia et al., 2019; Tieng et al., 2019). Given the fact that Landsat imagery and Sentinel imagery represent the two predominant

long-term remote sensing data in the public domain, it is worthwhile to compare their mapping performance despite their respective spectral, spatial, and temporal resolution.

To summarize, the objective of this study is to create a suitable method for mapping large-scale mangrove forests. Corresponding to the aforementioned three challenges, the particular objectives of this study include three aspects: (1) To automatically collect sufficient training samples for large-scale mangrove mapping; (2) To find a suitable classification method for large-scale mangrove mapping; (3) To compare the effectiveness of our classification method with different training samples, data sources and classifiers in different locations.

2. Study areas and data

2.1. Study areas

In order to test the reusability of our methods, two typical study sites were selected: the coastlines of Florida, the United States and the coastlines of Guangxi, China. Distribution patterns, species diversity and land cover adjacent to mangrove forests in the two locations are completely different. In Florida, mangrove forests cluster in large patches. There are three major mangrove species (*Avicennia germinans*, *Laguncularia racemose* and *Rhizophora mangle*), the height of which are from 9 m to 12 m (Feliciano et al., 2017). Conversion of mangrove forests to impervious areas or ponds rarely happens there, as the Everglades National Park has provided protection for about 76% mangrove forests in Florida since 1947 (Feliciano et al., 2017; Simard et al., 2006). Thus, a great amount of mangrove forests is adjacent to other types of forests. Alternatively, in Guangxi, mangrove species are more diverse: 15 species are found (Zhang et al., 2007). Eight species dominate there: *Avicennia marina*, *Aegiceras corniculatum*, *Kdel*, *Rhizophora stylosa*, *Bruguiera gymnorrhiza*, *Excoecaria agallocha*, *Acanthus ilicifolius* and *Heritiera littoralis* (Liang, 2000). The average heights for most of them are less than 3 m (Jia et al., 2014b; Li, 2004). Different from mangroves in Florida, a lot of mangrove forests in Guangxi are surrounded by ponds and artificial constructions, due to conversions of mangrove forests to aquaculture from 1980 to 2008 (Fan and Wang, 2017). Therefore, we selected Florida and Guangxi to test our methods in two different situations. Only coastal areas of the two study sites were considered, since mangrove forests are found along coastlines. Coastal areas were delineated according to the administrative boundaries of the United States and China. 20-km buffer zones for the coastlines were created as our study areas (Fig. 1).

2.2. Datasets

In order to get the recent status of mangrove forests in our study areas, we tested our methods by mapping the distribution of mangrove forests for the year 2018. A detailed description of the data for training sample collection, the data for classification, and the auxiliary data were introduced in the following three paragraphs respectively.

For training sample collection, the MFW and the time-series Landsat 5 and 8 surface reflectance images from 2000 to 2018 were used. Taking MFW as a base map, Landsat images were used to collect mangroves unchanged from 2000 to 2018. The MFW from the year 2000 was downloaded from the UN Environment World Conservation Monitoring Centre website. All the Landsat images from the year 2000 to 2018 were obtained from Google Earth Engine (GEE) (Gorelick et al., 2017). In these Landsat images, pixels considered to be clouds were masked out according to the "pixel_qa" band, a Landsat band describing cloud condition in each pixel.

In mangrove classification, SAR, optical images and topographic information were considered. Mangrove forests are evergreen forests having distinctive phenology. Thus, time-series SAR and optical images were utilized. In addition, topographic information was used to further exclude regions where mangrove forests unlikely occur, such as regions with high elevation or on a steep slope. To be more specific, the effect of Sentinel-1, and two commonly used optical data, Landsat 8 surface reflectance products and Sentinel-2 surface reflectance products (abbreviated as Landsat 8 and Sentinel-2, hereafter), were tested to find a good data combination for large-scale mangrove mapping. In addition, the 30-m Shuttle Radar Topography Mission (SRTM) digital elevation data and their derived variable (slope) were used to provide topographic information. Sentinel-1, Landsat 8, and SRTM were all obtained via GEE. However, the surface reflectance products of Sentinel-2 do not cover our study areas in 2017 and most months of 2018. We did atmosphere correction for the Sentinel-2 top-of-atmosphere products from GEE using a 6S radiative transfer model (Wilson, 2013). The code published by

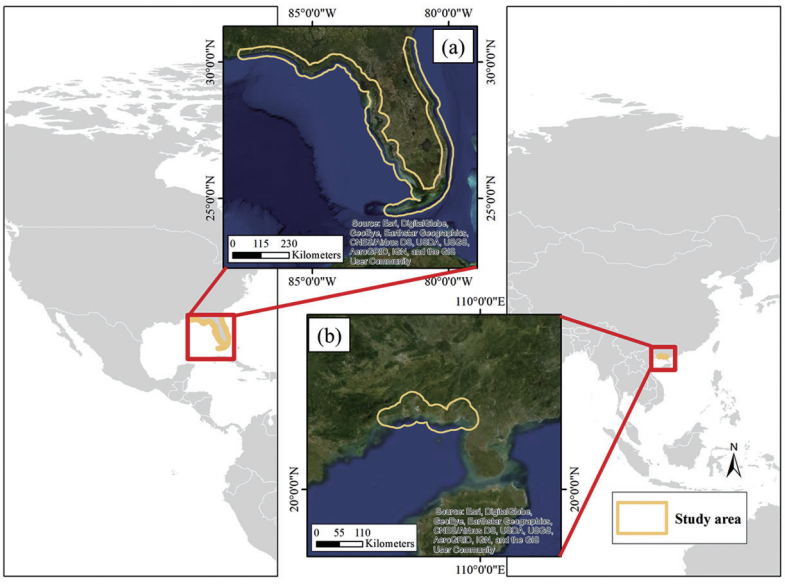

Fig. 1. Location of study areas: (a) Florida. (b) Guangxi.

Murphy and Hård (2017) was utilized. Moreover, the Sentinel-2: Cloud Probability dataset in GEE was used to remove clouds in Sentinel-2 with a manually selected threshold 50%, while clouds in Landsat 8 were masked out using the quality band, "pixel_qa". To further eliminate the influence of clouds, features were collected when the Normalized Difference Vegetation Index (NDVI) (Rouse et al., 1974) achieved the median and the maximum for each pixel in each season (Spring: March to May, Summer: June to August, Autumn: September to November, and Winter: December to the next year February). Nevertheless, after the elimination of clouds, the remaining data was not complete for Spring and Winter. Therefore, we assumed that the spatial extent of mangrove forests did not change significantly during three consecutive years. Additionally, data in Spring and Winter were combined as one season. Thus, Landsat-8, Sentinel-2 and Sentinel-1 in 2017, 2018 and 2019, and SRTM were collected to map the distribution of mangrove forests in 2018.

In addition, several auxiliary data were utilized in delineating the potential mangrove areas and validating our results. The administrative boundary maps of the United States and China were used to define coastlines. The GMW for the year 2016 was used as a reference to validate our results. Lastly, in order to evaluate the accuracy of our results, we visually interpreted 1533 non-mangrove and 541 mangrove points in Florida, and 1499 non-mangrove and 451 mangrove points in Guangxi, according to Google Earth Images.

3. Methods

The experimental design is shown in Fig. 2: Step 1, automatic training sample collection; Step 2, phenology-based feature extraction; Step 3, one-class classifiers; Step 4, knowledge-driven post-classification processing.

3.1. Automatic training sample collection

In this section, we proposed a new method to automatically collect training samples for large-scale mangrove mapping. Using the MFW from the year 2000 as a baseline, a rigorous screening process was utilized to collect unchanged areas from 2000 to 2018. Then, a region growing method was applied on the unchanged areas to increase the amount and the diversity of our training samples. Samples collected from the unchanged areas and the expanded areas were named as the unchanged training samples and the expanded training samples, respectively.

3.1.1. Unchanged training samples

The unchanged mangrove areas from the year 2000 to 2018 were collected according to annual maximum NDVI values, spatial characteristics and median NDVI values in 2018. Mangroves with diverse annual NDVI values from the year 2000 to 2018 were discarded. During this process, annual maximum NDVI values were collected for each mangrove pixel from 2000 to 2018, except 2012, because Landsat 5 and 8 images were incomplete in 2012. Therefore, 18 NDVI values were collected for each pixel. Standard deviation of these time-series NDVI values was used to evaluate the change. Pixels with standard deviation values greater than the average were considered having high potential to have changed. We discarded them as the first step of unchanged mangrove detection. This is because a great part of the changes in mangrove forests were caused by human activities, sea-level rise and soil erosion (Thomas et al., 2017). Mangrove forests were transformed into ponds, bare soil and open sea areas, leading to a significant decrease in NDVI. Then, spatial characteristics of mangrove pixels were considered. In fact, the major change factors for mangrove forests had a high probability to develop along boundaries. In order to ensure a high user's accuracy of the unchanged areas we collected, mangrove regions acquired from the previous step were shrunken 60 m inside. Finally, for median NDVI values in 2018, pixels within the first 2 percentiles were discarded to reduce errors inherited from the MFW. The MFW was not a 100% accurate product. In order to exclude the incorrect mangrove pixels in it, we used the median NDVI in 2018 to remove non-vegetation pixels in the unchanged areas. After these three steps, changed and misclassified areas were discarded from the MFW. This ensured that the delineated areas were the mangrove forests unchanged from 2000 to 2018. Almost all the three steps were implemented in GEE. We have shared the GEE code of deriving time-series NDVI values in the following

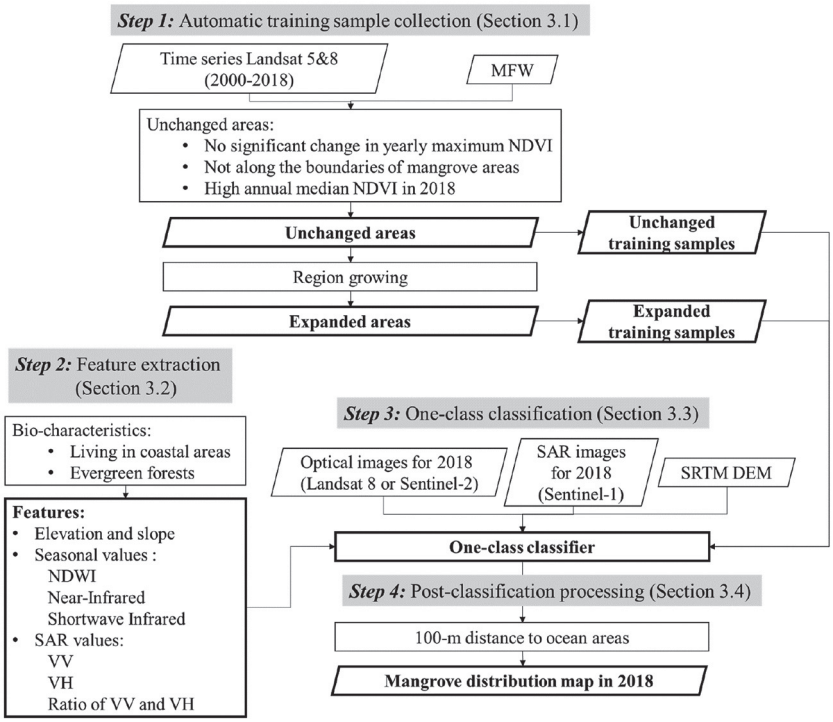

Fig. 2. Flow chart of the proposed approach.

link: https://code.earthengine.google.com/775c5b125daaac0c5514dc591e6e9877 .

3.1.2. Expanded training samples

A region growing method was used to expand the unchanged areas. As the detected unchanged areas were in the centers of mangrove patches, these areas were homogeneous and not able to completely describe the variance of mangrove forests. The unchanged training samples collected from these areas lacked mangrove pixels mixed with other land cover types and pixels for newly planted mangrove species. Therefore, region growing was used to solve this problem. The unchanged areas were used as seed pixels. For each pixel, their Green, Red, Near Infrared (NIR) and Shortwave Infrared (SWIR) bands' median and max values in 2018 were collected as input features. Seed pixels spatially connected were grouped together as seed regions. Mean feature values were calculated for each region. Euclidean Distance from each seed to the mean values were calculated in feature space. Through trial and error, 1.02 times of the 98th percentile distance value was used as a threshold to grow the region. Adjacent pixels of each seed region were absorbed into the region when their distances to the mean feature values were less than that threshold. Growing iterations and the number of new seeds were tracked for each time. Growing iterations were limited to ten. In addition, when the number of new seeds was less than 10% of the largest number in previous iterations or there were no pixels satisfying the requirement, the growing process for that region stopped. After the region growing process, mangrove regions we created were considered as expanded areas. The unchanged training samples, and the expanded training samples were randomly selected in the unchanged areas, and the expanded areas separately to analyze the impact of region growing on mangrove mapping. As it was difficult to implement in GEE, the region growing method was implemented in Matlab, while GEE was used to prepare the mean feature values.

3.2. Phenology-based feature extraction

In order to effectively delineate the distribution of mangrove forests, features should clearly distinguish mangrove forests from other land cover types. They were selected according to the bio-characteristics and the structure of mangrove forests. Optical features, SAR features, and elevation and slope were the three types of features (Table 1, Table 2) selected for our mangrove classification. As GEE provided almost all the datasets we needed except the Sentinel-2 surface reflectance products, the entire feature extraction work was implemented in GEE.

The optical features included seasonal NIR band values, seasonal SWIR band values and seasonal Normalized Difference Moisture Index values (NDWI, Eq. (1)) (Gao, 1996). Vegetation and non-vegetation have significant differences in NIR band, and SWIR bands. In addition, as tides move along coastal regions, a commonly used water index, NDWI, was utilized to distinguish mangrove areas from other inland forests. Moreover, seasonal trajectory information (seasonal values for each optical index) was used to describe the evergreen characteristic of mangrove forests. The aforementioned features were collected for every seasonal period when NDVI values were median and maximum.

The SAR features consisted of VV, VH and ratio of VV and VH. Their median and maximum values in 2018 were collected. SAR images are effective when clouds block optical information on the ground. Thus, in recent years, SAR images were considered as complementary data resources in mangrove mapping studies (Bunting et al., 2018; Chen et al., 2017; Thomas et al., 2018; Wang et al., 2019). They provide structural information on the ground's surface and are not affected by clouds. Their effects were analyzed in our study by investigating different performances of mangrove classification models with or without the SAR features.

Lastly, elevation and slope were considered. Since mangrove forests grow on flat terrain with low elevation, elevation and slope information are capable of differentiating mangrove forests from highland land covers. The three kinds of features mentioned above were uniformed with min-max normalization (Eq. (2)) in which the maximum and minimum values were collected from training samples.

$$NDWI = (\rho_{NIR} - \rho_{SWIR})/(\rho_{NIR} + \rho_{SWIR}) \quad (1)$$

$$X' = (X - X_{min})/(X_{max} - X_{min}) \quad (2)$$

Table 2
Features collected from SAR images.

	VV	VH	VV/VH
Yearly median value	√	√	√
Yearly maximum value	√	√	√

3.3. One-class classifiers

In the process of training sample collection, only mangrove training samples can be obtained automatically at large scales. Traditional multi-class supervised classifiers are unsuitable here. Thus, one-class classifiers, which only need us to label samples for a target land cover in training sample collection, were used in this study (Muñoz-Marí et al., 2007; Tax and Duin, 1999b).

Based on the characteristics of training samples, one-class classifiers can be classified into two groups: classifiers learned with target samples only, and classifiers learned with target samples and unlabeled ones. In order to test their performance in large-scale mangrove mapping, we discussed one typical classifier for each group: the Support Vector Data Description (SVDD) (Tax and Duin, 1999b) for the first group and the Positive and Unlabeled Learning algorithm (PUL) (Elkan and Noto, 2008; Li et al., 2010) for the second.

3.3.1. Support vector data description

Since the classification features were selected according to the bio-characteristics and the structure of mangrove forests, mangrove pixels were assumed to congregate in feature space. Therefore, SVDD, a one-class classifier similar to support vector machine, was suitable here (Muñoz-Marí et al., 2007; Tax and Duin, 1999b). This method only requires training samples for the target land cover type which is mangrove in this study. It aims to find a hypersphere with minimum volume which contains all, or most of, the training samples. This hypersphere is described with a center a and a radius $R > 0$. Training samples on the boundary of the hypersphere are support vectors. A training dataset with n samples $\{x_i\}_{i=1,2...n}$ should satisfy the requirements in Eq. (3).

$$\begin{aligned} &\min R^2 + C\Sigma\xi_i \\ &\text{s.t.} ||x_i - a||^2 \le R^2 + \xi_i, \xi i \ge 0 \forall i \end{aligned} \quad (3)$$

In order to remove outliers, slack variables $\{\xi_i\}_{i=1,2,...n}$ are introduced

Table 1
Features collected from optical images and SRTM.

	NDVI is maximum				NDVI is median				Elevation	Slope
	NDWI	NIR	SWIR1	SWIR2	NDWI	NIR	SWIR1	SWIR2		
Spring & Winter	√	√	√	√	√	√	√	√	√	√
Summer	√	√	√	√	√	√	√	√		
Autumn	√	√	√	√	√	√	√	√		

in SVDD. The penalty parameter C defines a trade-off between the simplicity of the sphere and the number of outliers. These parameters were set according to the study of Tax and Duin (1999b).

3.3.2. Positive and unlabeled learning algorithm

Besides mangrove samples, PUL tries to extract information from unlabeled sample points (Elkan and Noto, 2008; Li et al., 2010). It calculates the probability for each pixel to be labeled using mangrove training samples which are also considered to be labeled samples, and unlabeled samples randomly collected in study areas. Then, the probability for each pixel to be mangrove was derived. It aims to solve the function (4).

$$f\ (y=1|x) = N \times p(s=1|x) \big/ \Sigma_{x\in\{Mangrove\ Samples\}}\ p(s=1|x) \tag{4}$$

where $f\ (y=1|x)$ represents the probability that a pixel is mangrove. Only pixels with $f\ (y=1|x) \geq 0.5$ are recognized as mangrove forests. The threshold is set according to the study of Li et al. (2010). x is feature values for each pixel, and $y \in \{-1,1\}$ represents the land cover of a pixel: If $y=1$, the pixel is mangrove forests. Otherwise, the pixel belongs to other land cover types. N represents the number of mangrove training samples we collected. $p\ (s=1|x)$ is the probability for a pixel to be labeled. $s \in \{-1,1\}$ represents a pixel is unlabeled or labeled as mangrove forests respectively. Therefore, the PUL algorithm is able to be used with multi-class classification methods that can offer a probability for each pixel to be labeled. In this study, the PUL was implemented with a maximum likelihood classifier.

3.4. Knowledge-driven post-classification processing

After the one-class classification, mangrove regions in the results were selected by their distances from the ocean, as mangrove forests grow in intertidal areas. In the classification results, mangrove pixels adjacent to each other were clustered as mangrove regions. Regions touching the 100-m buffer of ocean regions were considered as the resultant mangrove distribution map for the year 2018 (Chen et al., 2017). Water bodies were mapped by pixels with a yearly median value of the Modified Normalized Difference Water Index (MNDWI, Eq. (5)) in 2018 greater than 0. This MNDWI was proven to be effective in delineating water boundaries by Xu (2006). The largest water region was considered as the major ocean extent. However, bays or estuaries separated by bridges were excluded from this extent. In the meantime, the major ocean extent contained a lot of ponds. Thus, we shrank the identified major ocean extent by 30 m. Water regions within 100-m distance from the shrunken areas were recognized as ocean regions.

$$MNDWI = (\rho Green – \rho SWIR)/(\rho Green + \rho SWIR) \tag{5}$$

3.5. Comparison of different classification models

For our proposed mangrove classification method, the selections in classification factors (training samples, data sources and classifiers) are significant for the results. Additionally, with the same factors applied, the results can be different in different study sites. Thus, it is essential for us to find a suitable combination of these factors to deal with different mapping requirements. In this study, five factors were considered: training data, optical data, inclusion of SAR, classifiers, and study sites.

The quality of training samples is critical for our proposed mapping method. In this study, two types of training samples, the unchanged training samples and the expanded training samples, were considered. Including newly planted mangrove pixels and pixels which are mixtures of mangroves and other land covers, the expanded training samples were expected to improve the accuracy of mangrove classification. However, the effectiveness of the region growing strategy had not been tested. It is meaningful to compare the training samples collected from the unchanged areas and the expanded areas.

The performance of our proposed mapping method is contingent upon the input optical data. Generally, mangrove forests are often distributed as elongated patches. Additionally, in comparison to other deciduous forests, they are evergreen forests with little phonological changes. In order to make use of this information, Landsat 8 and Sentinel-2 are commonly used in mangrove mapping (Chen et al., 2017; Giri et al., 2011). They are complementing as Landsat has full temporal coverage ranging from 1972, while Sentinel-2 has refined temporal, spectral and spatial resolutions. Therefore, it is worthwhile to investigate how resolutions play a role in the resulting mangrove maps.

The inclusion of SAR may impact the accuracy of our proposed mapping method. Compared with inland forests, mangrove trees are relatively smaller. Thus, their surface textures in remote sensing images are smoother, making mangrove forests distinctive in structure. The SAR information of Sentinel-1 imagery offers structure information of the land surface. In addition, it is not affected by clouds which often appear in mangrove areas. In recent years, some studies have used it to benefit their mangrove mapping (Chen et al., 2017; Tieng et al., 2019). Therefore, investigating the impact of SAR on our mangrove mapping method is helpful.

Different classifiers can generate different classification results. In this study, two typical one-class classifiers (SVDD and PUL) were analyzed. SVDD only needs mangrove training samples, while PUL requires randomly collected points in our study areas in addition to the mangrove training samples. In order to find which one-class classifier is suitable for our mangrove mapping method, it is worth comparing their performance.

Lastly, in different study sites where species and distribution patterns of mangrove forests are not the same, the performance of our proposed mangrove mapping method may be different. In this study, two study sites with distinctive mangrove species and distribution patterns, Florida and Guangxi, were studied. In Florida, mangrove patches are large and close to each other. A large part of coastal areas is covered by forests and impervious surfaces. In Guangxi, mangrove forests are sparsely distributed as small patches. Mangrove species are diverse there. Land cover along the coastlines varies, such as ponds, farmlands, impervious surfaces, and forests. In order to have a comprehensive understanding of our mangrove mapping method, it is meaningful to test it in the two study sites.

In summary, in order to analyze the influence of different factors, 16 mangrove classification models (Fig. 3) were trained for each study site (Florida and Guangxi) with two different training samples (the unchanged training samples or the expanded training samples), two different optical data sources (Landsat 8 or Sentinel-2), inclusion or exclusion of SAR, and two different one-class classifiers (SVDD or PUL). In total, 32 classification models were created. Due to the lack of required functions in GEE, we trained our models in Matlab. In addition, mangrove classification using PUL was also implemented in Matlab, while classification using SVDD was in GEE.

4. Results

4.1. Training sample collection

The unchanged areas of mangrove forests were detected based on Landsat 5 and 8 images from 2000 to 2018 and the MFW. After region growing, the expanded areas were created. The two kinds of areas were compared with the MFW in 2000 and the GMW in 2016 (Fig. 4). We found that the unchanged areas are located in the center of mangrove patches. The expanded areas not only include the mangrove forests along boundaries (Fig. 4a, c), but also include mangrove areas which were omitted by MFW (Fig. 4b, d). However, in the meantime, the expanded mangrove areas have more non-mangrove pixels (Fig. 4d) than the unchanged areas.

The total area of our expanded areas is 89,813,358 m^2 for Florida and 5,139,548 m^2 for Guangxi. To assess the accuracy of our training

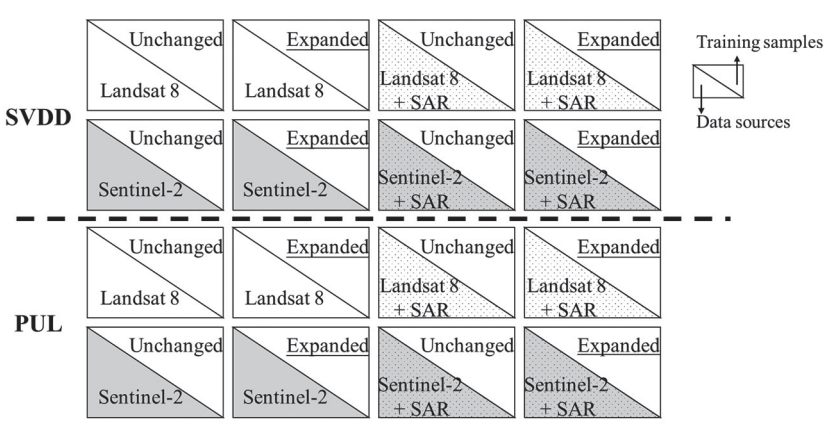

Fig. 3. 16 mangrove classification models for each study site. These models have different selection in the following four variables: training samples (unchanged or expanded training samples), optical data sources (Landsat 8 or Sentinel-2), inclusion or exclusion of SAR, and classifiers (SVDD or PUL).

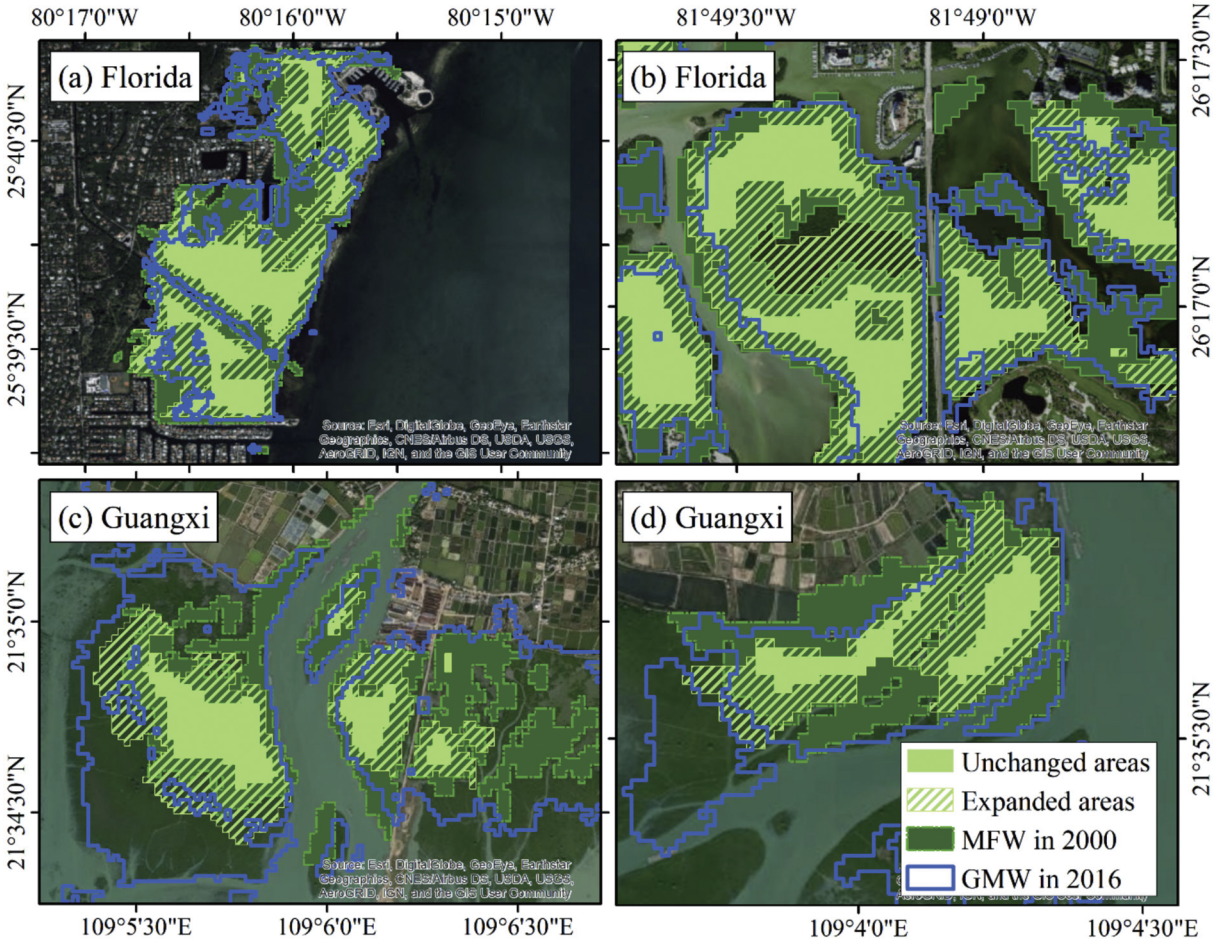

Fig. 4. Comparison of the derived training sample areas (the unchanged areas and the expanded areas), MFW for the year 2000 and GMW for the year 2016.

sample collection method in Florida, we visually interpreted 150 random points in the unchanged areas among which only 1 point was mislabeled, and 250 random points inside the expanded areas among which only 7 pixels were mislabeled. For Guangxi, 100 random points in the unchanged areas and 200 random points in the expanded areas were visually interpreted. User's accuracy for the unchanged areas and the expanded areas were 99.00% and 98.00% correspondingly. Finally, in order to test the effects of region growing, we randomly collected the unchanged and the expanded training samples from the unchanged areas and the expanded areas to train our classification models separately. The amount of training samples for Florida and Guangxi are listed in Table 3.

4.2. Classification results

According to Fig. 3, 16 mangrove classification models were created

Table 3
Numbers of training samples collected for Florida and Guangxi.

	Florida	Guangxi
Unchanged training samples	10,000	1813
Expanded training samples	20,000	6283
Unlabeled samples	40,000	16,000

for Florida and Guangxi separately (32 in total). Their accuracies can be found in Table S1. The overall accuracies for models in Florida range from 87.75% to 91.56%. For Guangxi, the range is from 89.64% to 96.92%. In both study sites, the highest overall accuracy was generated by the model using the unchanged training samples, PUL, Sentinel-1 SAR and Sentinel-2. This model can clearly differentiate mangrove forests from water, urban areas, soil, and a large number of inland forests. According to Fig. 5 (a, b) and Fig. 6 (a, b), the resultant mangrove extent can match GMW for the year 2016. In addition, some areas mislabeled by GMW are also correctly classified in our resultant maps. However, there are still some mistakes. This model omits some mangrove forests with few leaves (Fig. 5c) and sparsely distributed mangrove forests (Fig. 6c) which may be caused by sea-level rising, human deforestation and hurricanes. Additionally, evergreen forests distributed adjacent to coastlines (Fig. 5d) and vegetation growing along boundaries between two ponds (Fig. 6d) are possible to be misclassified as mangroves.

In order to better understand the impacts of the five factors (training samples, optical images, inclusion of SAR, classifiers, and study sites) on mangrove mapping, we summarized the results in the following five sections. In each section, only one factor is compared or evaluated. The 32 mangrove classification models are categorized into two groups referring to their selection in the considered factor no matter what we chose in the other four. For each group, a box plot for the overall, producer's, and user's accuracies of the mangrove maps made by these models are plotted.

4.2.1. *Different training samples*

To analyze the impact of training samples, we separated the 32 mangrove classification models into two groups: 16 models trained with the unchanged training samples, and 16 models trained with the expanded training samples. Within each group, the 16 models are mangrove classification models with different combinations of the four factors: optical data sources (Landsat 8 or Sentinel-2), inclusion of SAR (inclusion or not), classifiers (SVDD or PUL), and study sites (Florida or Guangxi). Fig. 7 shows boxplots of the overall, producer's, and user's accuracies of models in each group. For each type of accuracy, the left boxplot represents accuracies for models trained with the unchanged training samples and the right boxplot represents accuracies for models

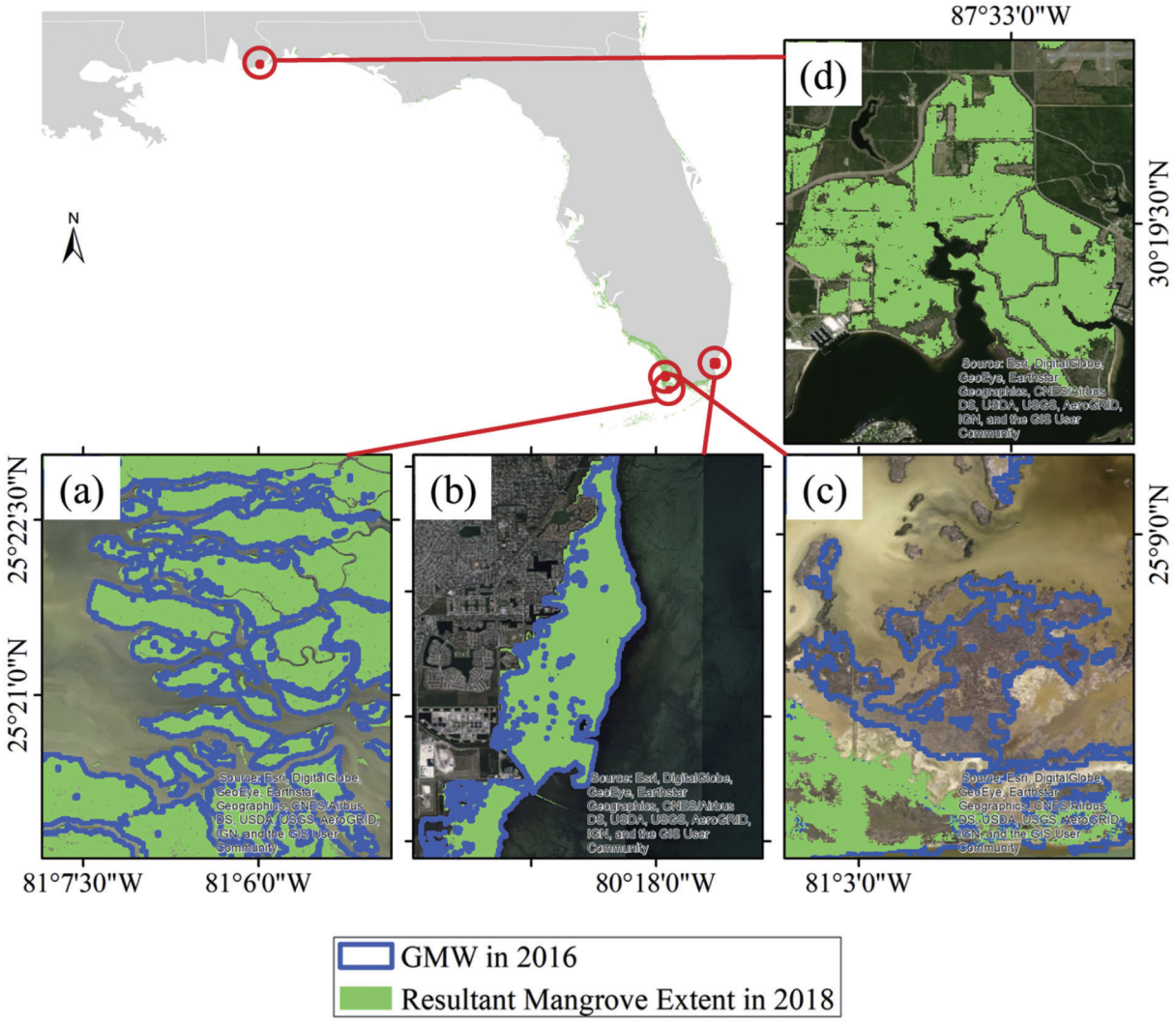

Fig. 5. The resultant mangrove map in Florida made by the model using the unchanged training samples, PUL, Sentinel-1 and Sentinel-2. (a, b) resultant mangrove extents consistent with GMW. (c) mangroves in GMW omitted by the resultant map. (d) evergreen forests in Florida misclassified as mangrove in the resultant map. All the 16 resultant maps in Florida can be accessed through the link: https://luyingGEEngine.users.earthengine.app/view/oneclassmangroveclassificationflorida

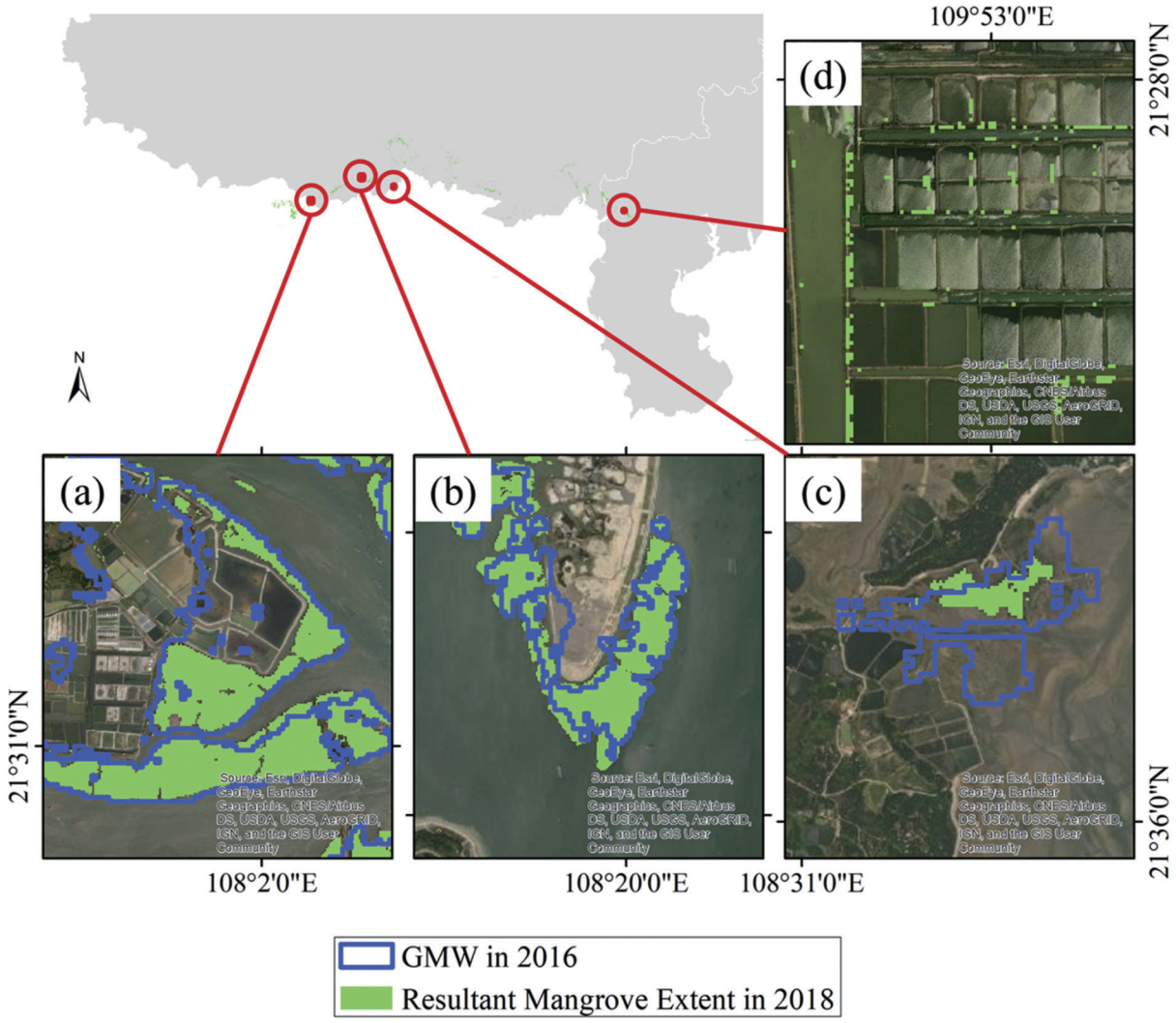

Fig. 6. The resultant mangrove map in Guangxi made by the model using the unchanged training samples, PUL, Sentinel-1 and Sentinel-2. (a, b) resultant mangrove extents more accurate than GMW. (c) sparsely distributed mangrove forests omitted by the resultant map. (d) vegetation along boundaries of ponds misclassified as mangrove in the resultant map. All the 16 resultant maps in Guangxi can be accessed through the link: https://luyingGEEngine.users.earthengine.app/view/oneclassmangroveclassificationguangxi

trained with the expanded training samples.

According to Fig. 7, changing training samples does not make significant differences on the overall accuracies of our classification models ($p = 0.052$, non-significant at 95% confidence level). The median overall accuracies of the two groups of models are almost the same (90.89% for models trained with the unchanged training samples; 90.74% for models trained with the expanded training samples). However, the differences between the two groups in the producer's accuracies and the user's accuracies are significant (producer's accuracies: $p = 0.005$; user's accuracies: $p = 0.008$). The most obvious contrast happens in the producer's accuracies. When we change the training sample source from the unchanged training samples to the expanded ones, the producer's accuracies increase and become more consistent (median value increased from 70.69% to 78.19%; variance decreased from 0.131 to 0.106). In contrast, the user's accuracies decrease and present greater variability (median value decreased from 93.47% to 90.59%; standard deviation increased from 0.053 to 0.076). This indicates that using the expanded training samples can help in recognizing more mangrove pixels at the cost of introducing more commission errors, i.e., more non-mangrove areas are classified as mangroves.

4.2.2. Different optical data

In this section, the performance of Landsat 8 and Sentinel-2 are compared. The 32 mangrove classification models are separated into two groups according to their optical data sources, Landsat 8 or Sentinel-2. The results of models in each group are summarized as boxplots in Fig. 8. For each type of accuracy, the left boxplot represents accuracies for models using Landsat 8 and the right boxplot represents accuracies for models using Sentinel-2.

Using different optical data causes significant differences in all the three types of accuracies (significant at 95% confidence level). In particular, the most significant one happens in producer's accuracy ($p = 0.003$). It is obvious that models using Sentinel-2 have higher and more constant producer's accuracies than models using Landsat 8. The median values of the producer's accuracies are 74.49% and 75.33%, and the standard deviations are 0.130 and 0.110 for models using Landsat 8 and Sentinel-2, correspondingly. In addition, when we changed the optical data from Landsat 8 to Sentinel-2, the overall accuracies have a slight improvement with the median value increasing from 90.16% to 91.68% while the standard deviation remains almost the same. By contrast, using Sentinel-2 has a negative effect on user's accuracy. Compared with models using Landsat 8, the user's accuracies of models using Sentinel-2 are smaller in general but have less variation. The median value

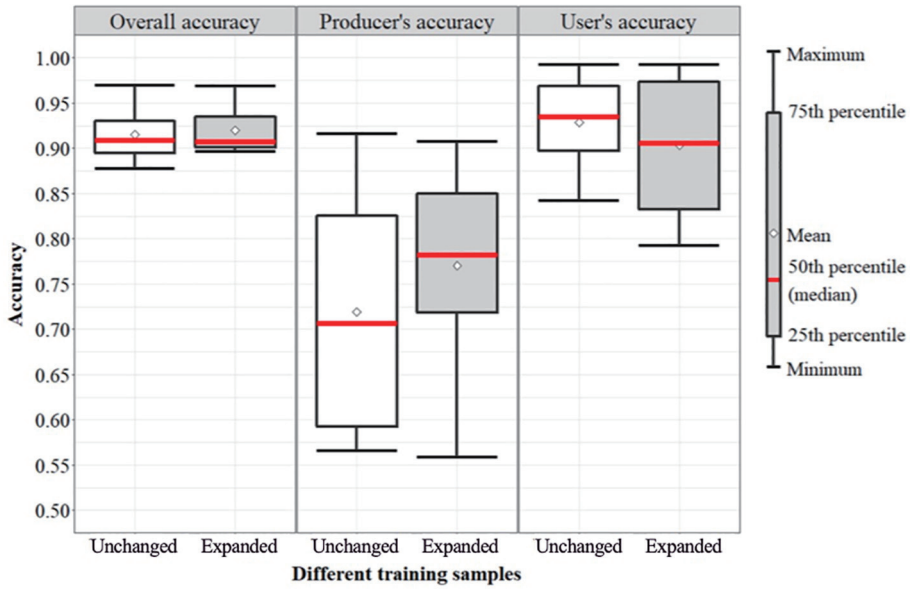

Fig. 7. Accuracies of mangrove mapping results using different training samples (the unchanged training samples or the expanded training samples).

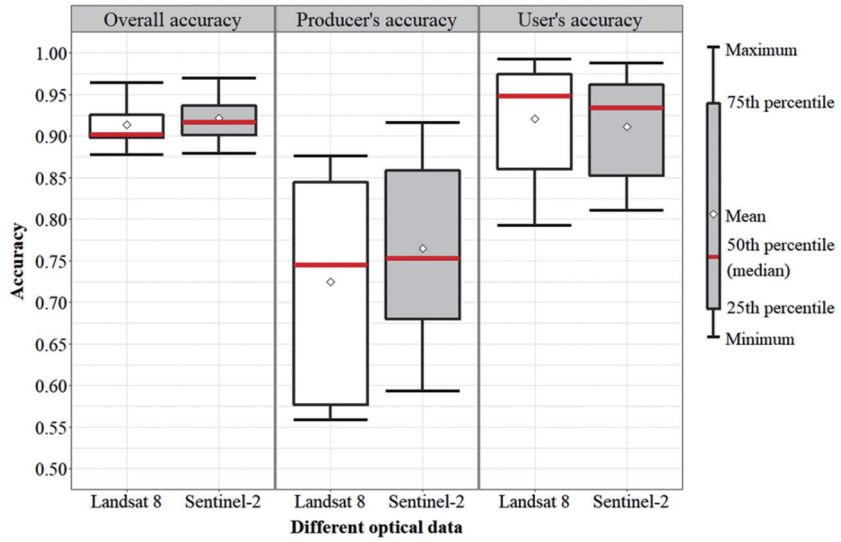

Fig. 8. Accuracies of mangrove mapping results using different optical images (Landsat 8 or Sentinel-2).

decreases from 94.85% to 93.38% and the standard deviation decreased from 0.068 to 0.065. In summary, compared with Landsat 8, Sentinel-2 makes the performance of mangrove mapping more stable and is effective in finding more mangrove pixels with the cost of introducing a few commission errors.

4.2.3. Inclusion of Sentinel-1 SAR data

The impact of SAR features is considered in this section. The mangrove classification models are divided into two groups: one using the SAR features extracted from Sentinel-1 images, and the other one does not. The results of each group are shown as boxplots in Fig. 9.

Even though all the three types of accuracies have improvements in mean and median values when we include SAR features in mangrove classification, the change is only significant in the overall accuracies and the producer's accuracies (overall accuracies: $p = 0.004$; producer's accuracies: $p = 0.018$; user's accuracies: $p = 0.188$). To be more specific, the median overall accuracy increases from 90.29% to 91.15%. The median producer's accuracy increases from 74.86% to 77.18%. Meanwhile, changes of standard deviation are less than 0.01 for both the overall accuracies and the producer's accuracies (standard deviation of the overall accuracies: increases from 0.029 to 0.030; standard deviation of the producer's accuracies: increases from 0.117 to 0.126). Thus, SAR features are effective in improving the performance of mangrove classification in most cases.

4.2.4. Different classifiers

Two one-class classifiers, SVDD and PUL, were compared in our study. The 32 models are classified into 2 groups: 16 models using SVDD and 16 models using PUL. In Fig. 10, the results of mangrove classification models in the two groups are summarized. Their overall, producer's and user's accuracies are all plotted as boxes.

The change of classifiers causes significant differences in all the three types of accuracies ($p \ll 0.001$). Models using PUL have a better performance in the producer's accuracies. Their producer's accuracies are higher and more constant. 50% of models using PUL have the producer's accuracies lying between 81.66% to 88.19%, while the respective values

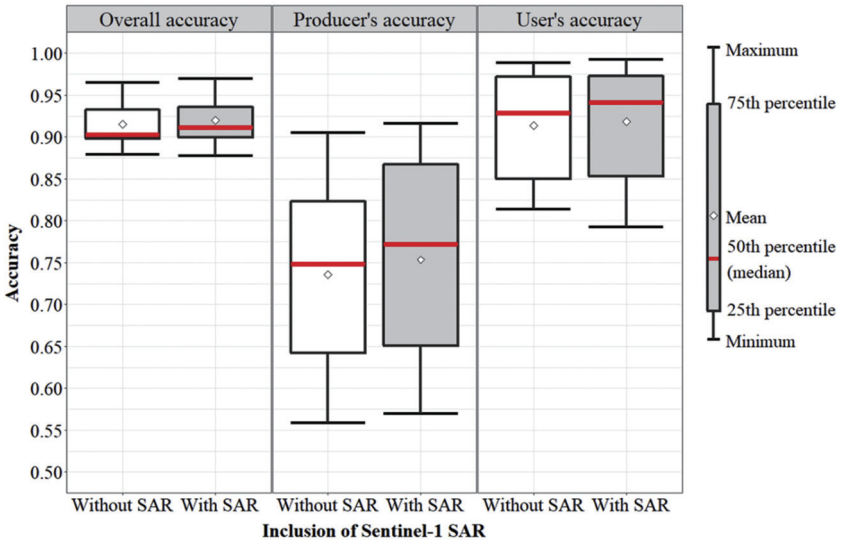

Fig. 9. Accuracies of mangrove mapping results with or without Sentinel-1 SAR.

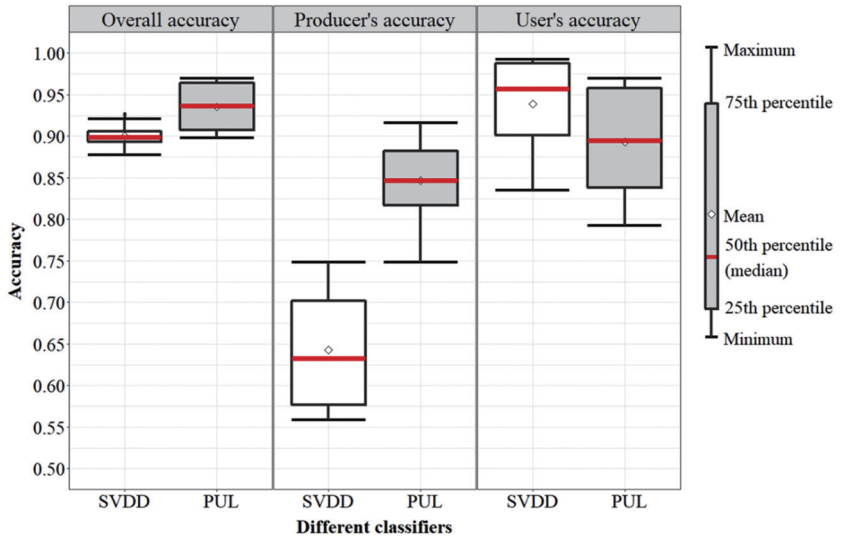

Fig. 10. Accuracies of mangrove mapping results using different one-class classifiers (SVDD or PUL).

of models using SVDD are 57.68% and 70.21%. Standard deviation of the producer's accuracies is 0.050 for models using PUL and 0.071 for models using SVDD. In contrast, the user's accuracies of models using PUL are more varied and smaller than that of models using SVDD. However, compared to the improvements that have been made by PUL in the producer's accuracies, the differences made in the user's accuracies are small. Thus, in the overall accuracies, models using PUL still have higher values while the variation is relatively higher. The range of the overall accuracies of the models using SVDD is 87.75%–92.72% while the range of the models using PUL is 89.78%–96.92%. Therefore, PUL classifier is effective in decreasing the omission errors in mangrove classification and, meanwhile, introduce a few commission errors.

4.2.5. *Different study sites*

In this section, the performance of our proposed mangrove mapping method is tested in two representative study sites: Florida and Guangxi. The results are summarized as boxplots in Fig. 11. Each boxplot contains accuracy values for 16 different classification models using different combinations in training samples (the unchanged training samples or the expanded training samples), optical data sources (Landsat 8 or Sentinel-2), inclusion of SAR (inclusion or not) and classifiers (SVDD or PUL).

The producer's accuracies of mangrove classification models are similar in Florida and Guangxi ($p = 0.515$, non-significant at 95% confidence level). They have similar median values (74.86% for Florida and 76.83% for Guangxi), while, for models trained for Guangxi, the producer's accuracies have a slightly wider range (57.12%–87.43% for Florida and 55.88%–91.57% for Guangxi). By contrast, the overall and user's accuracies have significant differences in the two study sites ($p \ll 0.001$). In Florida, the 16 mangrove classification models have smaller but more constant overall accuracies. The median value and the standard deviation of the overall accuracies for models in Florida are 90.07% and 0.012. For models in Guangxi, they are 94.23% and 0.029. The user's accuracies are higher and more consistent in Guangxi. Their median value and standard deviation are 97.48% and 0.018. In Florida, these values are 85.27% and 0.044. In summary, mangrove forests in Guangxi are more likely to be accurately delineated.

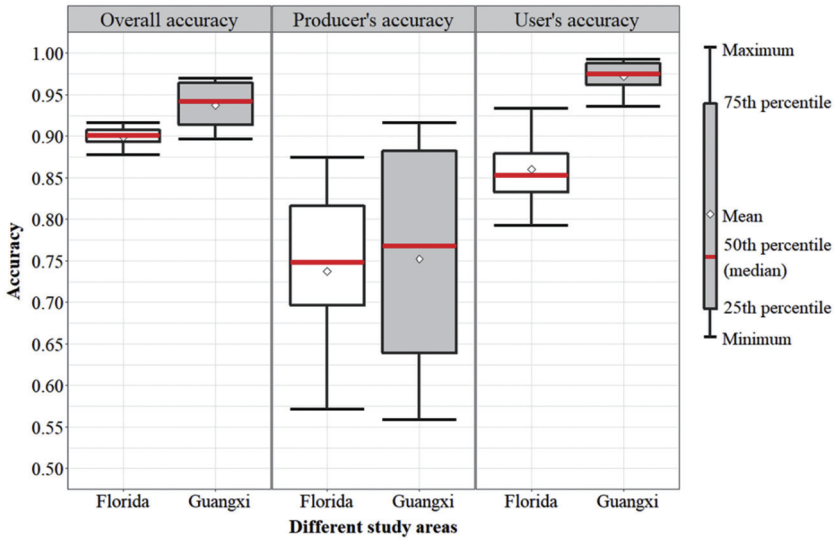

Fig. 11. Accuracies of mangrove mapping results in different study sites (Florida or Guangxi).

5. Discussion

In this paper, we developed an automatic training sample collection method. In addition, we found one-class classifiers can exploit the automatically derived mangrove training samples. By comparing the accuracies of our resultant mangrove maps generated by different models, we discovered that the expanded training samples are better than the unchanged training samples, Sentinel-2 outperforms Landsat 8 in most cases, utilizing SAR features collected from Sentinel-1 can improve the performance of mangrove classification, PUL is superior to SVDD. Additionally, our proposed mangrove mapping method performs better in study sites having diverse mangrove species than in where mangrove species are homogenous. To our knowledge, it is the first time that an automatic training sample collection method is developed for large-scale mangrove mapping. Our findings regarding the optimized combination of training samples, data sources, and classifiers adjusted for different study sites has shed some light on the implementation of timely large-scale mangrove mapping.

5.1. Merits of the developed methods for large-scale mangrove mapping

In this section, we aim to understand the merits of our developed methods in two aspects: training sample collection methods (Section 5.1.1), and classification methods (Section 5.1.2). Additionally, drawing upon the automation characteristics of our methods, we present the potential merits to apply our method for timely large-scale mangrove mapping (Section 5.1.3).

5.1.1. Automatic training sample collection

The proposed automatic training sample collection method is promising for solving the problem that training samples are lacking for timely large-scale mangrove mapping. It can be proven by the comparison with commonly used methods and the quality of training samples we collected for Florida and Guangxi.

Our proposed training sample collection method outperforms most methods in terms of labor-intensity. For previous large-scale mangrove mapping studies, training sample collection was an arduous task, despite the help of outdated maps. Visual interpretation and field works were widely used to generate up-to-date training samples from outdated maps, which required considerable time and expertise (Jia et al., 2018; Thomas et al., 2018). In contrast, no manual input is required to apply our method in future mangrove mapping tasks, although some manual work is involved in developing this method (e.g., defining region growing criteria). Two sets of mangrove training samples were collected: the unchanged training samples and the expanded ones. The unchanged training samples were collected by detecting unchanged mangroves in a historical map with two assumptions: the changed mangrove forests have large changes in inter-annual NDVI; boundaries of mangrove patches have a high possibility to change. With the help of GEE, which has an effective computation ability, we can automatically extract the unchanged training samples by eliminating mangrove pixels with large changes in inter-annual maximum NDVI and pixels locating inside a 60-m buffer zone of mangrove boundaries. In addition, in order to improve the diversity of training samples, the expanded training samples were collected by expanding the unchanged areas using a region growing method. We consider that pixels adjacent to the unchanged areas are also mangrove forests when they have similar spectra to the unchanged mangrove forests. Although some parameters were set through trial and error in this process, less human intervention is required in the future. Therefore, we believe our automatic training sample collection method is capable of collecting ample training samples in a timely manner, which can be broadly used in the future.

Additionally, the training samples collected by our method have high accuracy and diversity. According to Table 3, thousands of mangrove training samples were collected for both Florida and Guangxi. The user's accuracies for these training samples are all above 97%. Thus, for locations where there are mangrove forests unchanged from the year 2000 through 2018, mangrove training samples can be collected with high accuracy. In addition, the training samples can include most mangrove species in our study areas. For a certain mangrove species, if it has unchanged areas, it has a great chance to be collected. Moreover, mangrove species did not experience a large increase in the past two decades. The number of new species missing in our training data can be small. Thus, the training samples we collected are capable of describing most mangrove forests in our study areas. In sum, the amount, the accuracy and the diversity of our training samples can all satisfy the requirement of mangrove classification.

5.1.2. One-class classification applicable in large-scale mangrove mapping

Large-scale mangrove mapping greatly benefited from the one-class classification methods in our study. The one-class classification methods saved time and labor in training sample collection. In addition, it has the ability to accurately map the mangroves in Florida and Guangxi.

Compared with the commonly used multi-class classification methods, one-class classification improves the efficiency of mangrove mapping. This is because biodiversity is high in mangrove ecoregions. A

lot of land cover types, such as ponds, ocean, farmland, inland evergreen forests and deciduous forests, are inhabiting there (Spalding et al., 2010). It is difficult to timely collect ample training samples for multi-class classification at large scales. By contrast, one-class classification methods only require samples for the target land cover, which significantly relieves the requirements for training samples (Khan and Madden, 2014; Li et al., 2010; Tax and Duin, 1999b). In this study, SVDD only requires training samples for mangrove forests. PUL requires randomly collected samples in study areas besides mangrove training samples. With the help of our automatic training sample collection method, the process of training sample collection only costs a few hours. In addition, the computational complexity of one-class classifiers is similar to that of the commonly used classifiers, such as random forest and maximum likelihood. Therefore, one-class classification methods provide a new opportunity for large-scale mangrove mapping.

Additionally, one-class classification methods, especially PUL, are capable of mapping mangrove forests accurately. The overall accuracies of the 32 mangrove classification models are all above 80%. This is because SVDD aims to create a hypersphere with minimum volume which contains all the mangrove training samples. PUL aims to calculate the probability for each pixel to be mangrove. If representative features and training samples are selected, mangrove training samples will congregate in feature space, making it possible for one-class classifiers to delineate boundaries between mangrove forests and other land covers. In this study, we selected features according to the bio-characteristics of mangrove forests: living in low and flat intertidal zones and being evergreen vegetation. In these features, mangroves are distinctive from other land covers. Moreover, sufficient mangrove training samples were collected with high diversity using our automatic training sample collection method. Therefore, the phenology-based features and the high-quality training samples ensure the high performance of our one-class classification methods, making it feasible in large-scale mangrove mapping.

5.1.3. Timely large-scale mangrove mapping

The proposed mangrove mapping method has a great potential to be applied in timely large-scale mangrove mapping. We can understand it in three aspects: training data collection, one-class classifiers and the utilization of GEE. A comparison of our study and three typical large-scale mangrove mapping studies is listed in Table 4.

The automation of training sample collection is significantly promoted in this study, which enables us to timely generate training samples for large-scale mangrove mapping. Our training sample collection method is based on differentiating unchanged mangroves from changed ones in an existing historical map. For each study site, there are a lot of national, continental and global historical mangrove maps published, such as MFW and GWM, which can be used as base maps in training sample collection. Moreover, we used annual maximum NDVI to measure the change of mangrove forests, since the major change of mangrove forests, such as converting to water, soil or impervious surface, can cause large changes in it. The historical NDVI values for all the mangrove forests in the world can be obtained automatically from Landsat images in GEE. Thus, with the availability of base maps and historical NDVI values, our proposed mangrove training sample collection method can be applied in timely mapping mangrove forests at large scales.

In addition, implementing one-class classifiers in timely large-scale mangrove mapping is a promising prospect. As previously mentioned, one-class classifiers only require mangrove training samples. They save time in collecting training samples. In addition, the training and classification processes require little human intervention, which guarantees the automation of mangrove mapping. Moreover, the efficiency of mangrove classification is high for one-class classifiers. We only spent two days on generating the 32 mangrove maps in our study. Therefore, we believe one-class classification methods can be applied in timely mapping large-scale mangroves.

Lastly, GEE significantly improves the efficiency of image processing, which makes the timely large-scale mangrove mapping possible. It facilitates large-scale mapping by offering us a lot of ready-to-use remote sensing images, a great number of geo-processing functions and effective computation abilities(Gorelick et al., 2017; Wang et al., 2020). In this study, a large part of Landsat and Sentinel image processing work was implemented in GEE: generating annual NDVI standard deviation values for unchanged training sample collection, preparing input data for the classification models, classifying mangrove forests using SVDD and preparing MNDWI maps for the knowledge-driven post-classification processing. Although the region growing process, training of one-class classification models, and mangrove classification using PUL were implemented in Matlab, there are few parameters required to be determined manually. Thus, we believe, with further improvement our methods can be implemented entirely in GEE. In addition, thanks to GEE, ample representative training samples for Florida and Guangxi were automatically collected within only one to two hours, which was impossible in previous studies with visual interpretation or field works. About 1600 time-series Landsat 8 images and 13,177 time-series Sentinel-2 images were accessed in about 30 s. Features of 1000 to 20,000 widely scattered training samples were extracted for only 30 min. This is unimaginable before GEE became publicly available. Researchers had to download thousands of images from websites, mosaic them and pre-process these images with software in their own devices which consumed immeasurable time, labor and money. Therefore, GEE makes it easy and efficient for large-scale mapping, which is promising to be widely used in future studies.

5.2. Affecting factors on the mapping performance

In this study, training samples, data sources and study sites are considered as significant factors affecting the performance of mangrove mapping. Referring to our results, the mangrove classification model incorporating the unchanged training samples, PUL, Sentinel-1 and Sentinel-2 had the highest overall accuracy in both study sites. However, their user's accuracies are not the highest. This is because candidates in each factor have their own pros and cons. Different selections generate different mapping results. To provide recommendations for future studies, the five factors (training samples, optical data sources, inclusion of SAR, classifiers, and study sites) are discussed separately in the following five sections.

5.2.1. Training sample uncertainty

With regard to our comparison in training samples, the results do not align with what we expected. The expanded training samples do not improve the classification accuracy all the time. In this section, we

Table 4
Comparison of this study and three typical large-scale mangrove mapping studies.

	Giri et al. (2011)	Chen et al. (2017)	Thomas et al. (2018)	This paper
Training sample	No training sample	In situ data	Visual interpretation	Automatic method
Mangrove mapping methods	Hybrid supervised and unsupervised classification	Decision trees classification	Object-based random forests classification	One-class classification
Image pre-processing tools	Manually	GEE	Python	GEE and Matlab
Year of map	2000	2015	1996–2010	2018

compared the effects of the unchanged training samples and the expanded training samples for our classification models. According to Fig. 7, two major differences can be discerned.

In general, in comparison with models using the unchanged training samples, models using the expanded training samples have larger producer's accuracies and smaller user's accuracies. The unchanged training samples are composed of unchanged mangrove pixels in the geographic centers of mangrove patches, most of which are pure pixels. It may be difficult to recognize newly planted mangrove pixels and mangrove pixels mixed with other land covers using classification models trained by these samples. By contrast, the expanded training samples contain more mixed and newly planted mangrove pixels which are helpful to identify more mangrove pixels. Thus, the producer's accuracies of models using the expanded training samples are higher. Nevertheless, in the meantime, non-mangrove pixels sharing similar phenology-based features with these mixed and newly planted mangrove pixels are more likely to be included in our results. Therefore, the user's accuracies decline. Thus, the expanded training samples produced by region growing can improve producer's accuracies with the cost of user's accuracies.

For models trained with the expanded training samples, the producer's accuracies are more consistent while the user's accuracies have larger variation. This is because the mixed and newly planted mangrove pixels in the expanded training samples equip our classification models with the capability of recognizing enough mangrove forests, regardless of mangrove distribution patterns. In contrast, the performance of models using the unchanged training samples largely relied on the distribution patterns of mangrove forests. In locations where mangrove forests are diverse, sparsely distributed and mixed with other land covers, such as Guangxi, the unchanged training samples are diverse enough to represent the mangrove forests. Mangrove classification models trained with our two kinds of training samples have similar results. However, in locations where mangrove forests are clustered as large patches, such as Florida, almost all the unchanged training samples are pure pixels. Models trained with the unchanged training samples can omit a great number of mangrove pixels. Thus, the performance of models using the unchanged training samples is significantly different in different study sites. This may be the reason why the variation of producer's accuracies is large for models using them. However, we cannot ignore that, by introducing more mixed pixels, the expanded training samples increase the risk of mislabeling non-mangrove pixels as mangrove, which increases the diversity in user's accuracy. Thus, models using the expanded training samples are stable in recognizing mangrove forests in different study sites, while their capability in distinguishing non-mangrove forests is inconsistent.

5.2.2. Landsat 8 vs. Sentinel-2 data

With reference to the results of classification models using different optical images, Landsat 8 and Sentinel-2 have different impacts. Generally, Sentinel-2 outperforms Landsat 8 in the overall accuracies. However, their impacts on the producer's accuracies and user's accuracies are the opposite.

In general, the producer's accuracies of models using Sentinel-2 are larger than that of models using Landsat 8. Pixels in Landsat 8 imagery are more likely to be mixtures of mangrove forests and other land covers, as their spatial resolution is 30 m which is larger than that of Sentinel-2. These mixed pixels are mainly distributed along mangrove boundaries or in mangrove patches which are elongated. They may not be able to be classified as mangroves when the fractions of mangrove forests are not enough. In comparison, with higher spectral and spatial resolution, Sentinel-2 images can better detect the boundaries of land covers. These images divide a 30 * 30 m^2 region into nine 10 * 10 m^2 pixels. Mangrove forests missed by models using Landsat 8 are possible to be identified using Sentinel-2. Thus, using Sentinel-2 can improve the producer's accuracies by retrieving mangrove forests along mangrove boundaries and mangroves clustered as elongated patches.

Mangrove classification models using Landsat 8 have higher user's accuracies. When grasses or small trees grow along narrow boundaries between two water regions, their phenology-based features will be similar to that of mangrove forests. The widths of these boundary areas are mainly from five to twenty meters in our study areas. Thus, if we use Landsat 8 to divide the boundary areas into several 30 * 30 m^2 pixels, water fraction is very large in each pixel. Pixels containing grasses or small trees cannot be classified as mangroves. Nevertheless, in the same boundary areas, Sentinel-2 can generate a set of pixels with high fractions of grasses or small trees by dividing one Landsat 8 pixel into nine. Thus, grasses and trees along water boundaries are more likely to be classified as mangroves using Sentinel-2. This means that using Sentinel-2 can mislabel more non-mangrove land covers as mangrove forests.

5.2.3. Inclusion of SAR

In recent years, SAR features collected from Sentinel-1 have been used to benefit mangrove mapping studies (Chen et al., 2017; Tieng et al., 2019). It improved the performance of our proposed mangrove classification method generally. However, they can make a negative impact on the performance of models using SVDD. Thus, in this section, we analyzed the advantages of SAR as well as some exceptions.

Generally, when we include SAR in the classification, our classification models witness significant increases in the producer's accuracies, while the user's accuracies remain almost the same. This is reasonable because SAR offers structure information on the ground which cannot be obtained from optical images. Moreover, SAR images are capable of providing ground information when optical images are covered by clouds. Thus, using features derived from SAR, the classification models can recognize more mangrove forests than the ones not used. However, there was little change in the user's accuracies before and after using the SAR features. This may be caused by the fact that most mislabeled non-mangrove pixels in our study areas are land covers with high similarity to mangrove forests. It is plausible that the phenology-based features used in this study were not able to differentiate them from mangrove forests. Thus, the SAR features can improve the capability of mangrove classification models in recognizing more mangrove forests. However, to improve the user's accuracy of mangrove mapping, more effective features are required for future studies.

Nevertheless, for most models using SVDD to map the mangrove forests in Florida, the producer's accuracies decrease when SAR features are included. SVDD aims to create a hypersphere with minimum volume in feature space to include all the mangrove training samples inside. If the diversity of training samples is not high enough, they will be over-centralized in feature space. Consequently, the size of the hypersphere we create is less than the actual one. In this circumstance, the more features we provide, the smaller the hypersphere can be. Mangrove points outside the hypersphere will be excluded. Additionally, there are only three major mangrove species in Florida, which means that the diversity of training samples there is low. Thus, using SAR cannot improve the performance of SVDD classification in Florida. In summary, when the training samples are not diverse enough, increasing features for SVDD may cause the decline in classification accuracy.

5.2.4. SVDD vs. PUL

PUL is more suitable for large-scale mangrove mapping, according to the comparison of SVDD and PUL (Fig. 10). Although SVDD performs better in the user's accuracies, it is not recommended, since this classifier omits a large part of mangrove pixels in our study areas. About 35% to 45% of mangrove forests are missing on the mangrove maps generated by SVDD. In order to further understand the differences between these two classifiers, we discussed them in the following two aspects: the producer's accuracy and the user's accuracy.

Models using PUL have higher and more consistent producer's accuracies because they not only utilized mangrove samples, but also randomly collected samples which were not considered in SVDD. PUL aims to find a boundary between mangrove and non-mangrove pixels in

the feature space. Mangrove pixels which are very different from our mangrove training samples can be correctly recognized when these pixels are closer to mangroves than they are to non-mangroves in feature space. Some examples are mangrove pixels mixed with other land covers and pixels occupied by newly planted mangroves. Alternatively, SVDD aims to find a border of mangrove training samples in the feature space. Only pixels having high similarity to the training samples can be classified as mangrove forests. Thus, PUL can detect more mixed mangrove pixels than SVDD. The diversity of mangrove training samples has less influence on PUL. Therefore, by using randomly collected unlabeled pixels as a reference, the performance of PUL is better and more stable.

Meanwhile, the user's accuracies for models using SVDD are higher than that for models using PUL. For SVDD, only pixels close to the mangrove training samples in feature space are classified as mangrove forests. A large part of non-mangrove pixels can be correctly recognized by SVDD. Nevertheless, PUL calculates the possibility of pixels to be mangroves by comparing their distances to mangroves and non-mangroves in feature space. Thus, more non-mangrove pixels that are comparable to mangroves are misclassified by PUL. In summary, using SVDD, the resulting mangrove maps have high user's accuracies at the cost of omitting significant numbers of mangrove pixels.

5.2.5. Different study sites

Concerning our classification results, the performances of our mangrove classification models are distinctive in different study sites (Florida and Guangxi). Although the producer's accuracies do not experience significant changes when we change the study site, there are still changes we can witness when we take the classifier into account. Thus, in this section, we discussed the influence of study sites in two aspects: the user's accuracies and the producer's accuracies.

Generally, the mangrove classification models have better performance in mapping mangrove forests in Guangxi, with relatively higher user's accuracies and overall accuracies. A large part of the coastlines in Guangxi are covered by anthropogenic land covers, such as ponds, impervious surfaces and farmlands which are significantly different from mangrove forests in phenology features. In contrast, most land cover types along coastlines in Florida are vegetation. They are likely to have comparable phenology features with mangrove forests. Thus, in Guangxi, the mangrove classification models can better eliminate non-mangrove pixels.

When we analyzed the producer's accuracies in detail, we recognized that, in most cases, Guangxi witnesses higher omission errors than Florida when we use SVDD in mangrove classification models. In contrast, for models using PUL, omission errors in Guangxi are less than that in Florida. This is because mangroves in Guangxi are diverse and sparsely distributed. Florida only has three major mangrove species which are clustered as large patches spatially. Mangroves in Florida can be more concentrated in feature space. Thus, using SVDD, fewer mangroves are omitted in Florida than in Guangxi. Moreover, the primary land covers along coastlines in Guangxi are anthropogenic land covers having significant differences with mangroves, while most coastal areas in Florida are covered by vegetation. By comparing the distances from each pixel to mangroves and non-mangroves in feature space, it is easier for PUL to differentiate mangrove forests from other land covers in Guangxi than in Florida. However, what we need to know is that although the producer's accuracies of PUL decreased when we changed the study site from Guangxi to Florida, it still outperformed SVDD. In summary, even though the producer's accuracies increased for SVDD models when we changed the study site from Guangxi to Florida, PUL is still the best choice for both our study sites.

5.3. Limitations

Although our large-scale mangrove mapping method proved to be effective, we realize that three major limitations are still present before our method can be applied to timely mapping mangroves at large scales. These limitations reside in the training samples quality, the remote sensing data availability, and the post-classification processing, respectively.

5.3.1. Training samples

The quality of our training samples is attributed to three factors: the base map accuracy, the unchanged mangrove detection method, and the region growing method. In order to examine the training sample quality, we will discuss each factor regarding omission and commission errors. Omission errors are related to the fact that unchanged mangrove forests and newly planted mangrove forests are not fully collected. Commission errors refer to the fact that the mangrove training samples are contaminated by non-mangrove ones.

The omission and commission errors of the base map, MFW from the year 2000, propagate to our training samples. From visual inspection, we found that the base map omitted some small mangrove patches far from coastlines. Our two kinds of training samples, the unchanged and the expanded ones, were generated based on detecting unchanged mangroves from the year 2000 to 2018 in the base map. Thus, the mangroves omitted by the base map were also missed in our mangrove training samples, especially in the unchanged training samples. In addition, the commission errors of the base map resulted from the fact that some non-mangrove land covers, such as grass and inland forests, were mislabeled as mangroves. As a result, if the mislabeled mangrove pixels do not change from the years 2000 to 2018, it is possible to include these pixels in our training samples. Thus, the accuracy of the base map influences the accuracy of our training samples, which further influences the performance of our mangrove classification method.

The unchanged mangrove detection method was used to derive the unchanged training samples. However, it introduced omission and commission errors in the training samples. To ensure the selected areas were mangrove forests that were unchanged from 2000 to 2018, we discarded more than half of the mangrove pixels in our base map assuming that unchanged mangrove forests have small changes in annual maximum NDVI and have high potential to be located in the centers of mangrove patches. However, during the 19 years, mangrove forests did not change that much. Therefore, two types of unchanged mangrove pixels are omitted in the unchanged training samples: Mangrove pixels having heterogeneous NDVI values from 2000 to 2018, and mangrove pixels along boundaries of mangrove patches. If these omitted mangroves are different in phenology features from our training samples, the training samples will not be diverse enough to represent the mangrove forests in our study areas. In addition, the commission errors of the unchanged training samples resulted from the fact that we used the change of annual maximum NDVI to evaluate the change of mangrove pixels from the years 2000 to 2018. It is possible for changed pixels having homogeneous time-series NDVI values to be detected as unchanged ones. For example, if mangrove pixels are quickly replaced in one year by plants having similar NDVI to mangroves, the standard deviations of their annual maximum NDVI values will be small. Consequently, the changes will be neglected. These quick changes generally occurred along boundaries of mangrove patches, such as species invasion and human disturbance. Although we shrank the result of unchanged mangrove detection 60 m inside, the quickly changed pixels within the centers of mangrove patches still remained in our training samples.

Moreover, region growing brings in non-mangrove pixels to the expanded training samples. To increase the diversity of our training samples, pixels nearby the unchanged areas were considered as mangroves when they had similar spectra to mangrove forests. However, non-mangrove vegetation pixels, such as inland forests and ponds with aquatic vegetation, can also have similar spectral information with mangrove forests. When these pixels are next to the unchanged areas, they have a high potential to be collected. Moreover, parameters for the region growing method were manually selected through trial and test. Further research is required to determine these parameters more

automatically and to generate a more accurate result.

5.3.2. Data availability and quality

The availability of Sentinel-2 limits the scale and the accuracy of our mangrove mapping. To further prove the capability of our method for timely large-scale mangrove mapping, it should be tested in more locations with larger scales. However, the lack of global Sentinel-2 surface reflectance prohibits our ability to select more study sites.

Sentinel-2 surface reflectance products are not available globally for the year 2017 and 2018. Although Sentinel-2 surface reflectance products for these years are published by some platforms, such as the Sentinel-2 value adder (Vuolo et al., 2016), these data are not included in GEE. It is challenging or even impossible to download and analyze all of them in our study areas using our own devices. In this study, we used the 6S radiative transfer model and the GEE Application Programming Interface in python to do atmospheric correction for the 21,000 Sentinel-2 top-of-atmosphere images in our study sites, which took more than half of a month. Thus, it is hard for us to expand our study areas. Fortunately, surface reflectance products for Sentinel-2 have been globally available in GEE since 2019. Our proposed method shows promise for the capability of mapping mangrove forests globally in the foreseeable future.

5.3.3. Post-classification processing

Knowledge-driven post-classification processing removes inland mangrove patches and keeps non-mangrove forests close to the coastlines in our classification results. As mangrove forests were considered for distribution along coastlines, mangrove patches un-touching the 100-m buffer of the ocean were deleted from our one-class classification results. The ocean areas were mapped using MNDWI>0. However, shallow and muddy water areas are not fully delineated. Mangrove forests close to these shallow and muddy water areas are omitted. In addition, ponds close to coastlines are likely to be considered as ocean areas. As a result, ponds with aquatic vegetation and evergreen inland forests adjacent to these areas are likely to be misclassified as mangrove forests. Alternatively, a coastal tidal flat map can be used to restrict the distribution of mangrove forests. Mangrove forests are periodically flooded by tides; thus, they are close to intertidal regions in spatial distribution. Since GEE has become available, it is more convenient for researchers to access time-series Landsat and Sentinel imagery. In addition, automation and accuracy of tidal flat mapping have been improved in recent studies (Wang et al., 2020; Jia et al., 2021). Therefore, tidal flat maps have a high potential to improve the accuracy of our results.

6. Conclusion

The ability of carbon absorption, water purification and nutrient storage establishes the importance of mangrove forests. There is a desperate need to map the latest distribution of mangrove forests at large scales. In the meantime, the increasing number of time-series remote sensing images build the foundation for large-scale mangrove mapping. The cloud data processing platform, GEE, accelerates the procedure of mapping. This study developed an automatic training data collection method to collect ample training samples for large-scale mangrove mapping. In addition, it is the first time that one-class classifiers are used to map the distribution of mangrove forests at large scales. We analyzed the effects of different training samples, data sources, classifiers, and study sites in our proposed one-class mangrove classification method. The combination of Sentinel-1, Sentinel-2 and PUL showed a high performance. Moreover, it is undeniable that there will be a lot of work to be done to improve our study, such as finding more representative mangrove samples, testing our method in more locations and improving the accuracy of ocean areas.

Supplementary data to this article can be found online at https://doi.org/10.1016/j.rse.2021.112584.

Declaration of Competing Interest

The authors declare that they have no known competing financial interests or personal relationships that could have appeared to influence the work reported in this paper.

Acknowledgements

Many thanks to the editorial team of Remote Sensing of Environment and the 4 anonymous reviewers for their valuable insights and helpful suggestions. This work is supported by the National Science Foundation (Award #1951657).

References

Alongi, D., 2009. The Energetics of Mangrove Forests. Springer Science & Business Media BV.
Blaber, S.J.M., Milton, D.A., 1990. Species composition, community structure and zoogeography of fishes of mangrove estuaries in the Solomon Islands. Mar. Biol. 105, 259–267.
Bunting, P., Rosenqvist, A., Lucas, R.M., Rebelo, L.M., Hilarides, L., Thomas, N., Hardy, A., Itoh, T., Shimada, M., Finlayson, C.M., 2018. The global mangrove watch—a new 2010 global baseline of mangrove extent. Remote Sens. 10 (10), 1669.
Chen, X., Yin, D., Chen, J., Cao, X., 2016. Effect of training strategy for positive and unlabelled learning classification: test on Landsat imagery. Remote Sens. Lett. 7 (11), 1063–1072.
Chen, B., Xiao, X., Li, X., Pan, L., Doughty, R., Ma, J., Dong, J., Qin, Y., Zhao, B., Wu, Z., 2017. A mangrove forest map of China in 2015: analysis of time series Landsat 7/8 and Sentinel-1A imagery in Google Earth Engine cloud computing platform. ISPRS J. Photogramm. Remote Sens. 131, 104–120.
Denis, F., Gilleron, R., Tommasi, M., 2002. Text classification from positive and unlabeled examples. In: Proceedings of the 9th International Conference on Information Processing and Management of Uncertainty in Knowledge-Based Systems, IPMU'02, pp. 1927–1934.
Diniz, C., Cortinhas, L., Nerino, G., Rodrigues, J., Sadeck, L., Adami, M., Souza-Filho, P. W.M., 2019. Brazilian mangrove status: three decades of satellite data analysis. Remote Sens. 11 (7), 808.
Donato, D.C., Kauffman, J.B., Murdiyarso, D., Kurnianto, S., Stidham, M., Kanninen, M., 2011. Mangroves among the most carbon-rich forests in the tropics. Nat. Geosci. 4, 293–297.
Elkan, C., Noto, K., 2008. Learning classifiers from only positive and unlabeled data. In: Proceedings of the 14th ACM SIGKDD International Conference on Knowledge Discovery and Data Mining, pp. 213–220.
Fan, H., Wang, W., 2017. Some thematic issues for mangrove conservation in China. J. Xiamen Univ. 56, 323–330.
FAO, 2007. The World's Mangroves 1980–2005. FAO, Rome, Italy.
Feliciano, E.A., Wdowinski, S., Potts, M.D., Lee, S.K., Fatoyinbo, T.E., 2017. Estimating mangrove canopy height and above-ground biomass in the everglades national park with airborne lidar and tandem-x data. Remote Sens. 9 (7), 702.
Friedl, M.A., McIver, D.K., Hodges, J.C., Zhang, X.Y., Muchoney, D., Strahler, A.H., Schaaf, C., 2002. Global land cover mapping from MODIS: algorithms and early results. Remote Sens. Environ. 83 (1–2), 287–302.
Gao, B.C., 1996. NDWI—A normalized difference water index for remote sensing of vegetation liquid water from space. Remote Sens. Environ. 58 (3), 257–266.
Giri, C., 2016. Observation and monitoring of mangrove forests using remote sensing: opportunities and challenges. Remote Sens. 8 (9), 783.
Giri, C., Ochieng, E., Tieszen, L.L., Zhu, Z., Singh, A., Loveland, T., Masek, J., Duke, N., 2011. Status and distribution of mangrove forests of the world using earth observation satellite data. Glob. Ecol. Biogeogr. 20 (1), 154–159.
Giri, C., Long, J., Abbas, S., Murali, R.M., Qamer, F.M., Pengra, B., Thau, D., 2015. Distribution and dynamics of mangrove forests of South Asia. J. Environ. Manag. 148, 101–111.
Gorelick, N., Hancher, M., Dixon, M., Ilyushchenko, S., Thau, D., Moore, R., 2017. Google Earth Engine: planetary-scale geospatial analysis for everyone. Remote Sens. Environ. 202, 18–27.
Hamilton, S.E., Casey, D., 2016. Creation of a high spatio-temporal resolution global database of continuous mangrove forest cover for the 21st century (CGMFC-21). Glob. Ecol. Biogeogr. 25 (6), 729–738.
Hansen, M.C., DeFries, R.S., 2004. Detecting long-term global forest change using continuous fields of tree-cover maps from 8-km advanced very high resolution radiometer (AVHRR) data for the years 1982–99. Ecosystems 7, 695–716.
Islam, M.M., 2017. Tracing Mangrove Forest Dynamics of Bangladesh Using Historical Landsat Data. Lund University (INES NR415), Lund, Sweden.
Jia, M., Wang, Z., Li, L., Song, K., Ren, C., Liu, B., Mao, D., 2014a. Mapping China's mangroves based on an object-oriented classification of Landsat imagery. Wetlands 34, 277–283.
Jia, M., Wang, Z., Zhang, Y., Ren, C., Song, K., 2014b. Landsat-based estimation of mangrove forest loss and restoration in Guangxi province, China, influenced by human and natural factors. IEEE J. Select. Topics Appl. Earth Observ. Remote Sens. 8, 311–323.

Jia, M., Wang, Z., Zhang, Y., Mao, D., Wang, C., 2018. Monitoring loss and recovery of mangrove forests during 42 years: the achievements of mangrove conservation in China. Int. J. Appl. Earth Obs. Geoinf. 73, 535–545.
Jia, M., Wang, Z., Wang, C., Mao, D., Zhang, Y., 2019. A new vegetation index to detect periodically submerged mangrove forest using single-tide Sentinel-2 imagery. Remote Sens. 11 (17), 2043.
Jia, M., Wang, Z., Mao, D., Ren, C., Wang, C., Wang, Y., 2021. Rapid, robust, and automated mapping of tidal flats in China using time series Sentinel-2 images and Google Earth Engine. Remote Sens. Environ. 255, 112285.
Kathiresan, K., 2003. How do mangrove forests induce sedimentation? Rev. Biol. Trop. 51, 355–360.
Khan, S.S., Madden, M.G., 2014. One-class classification: taxonomy of study and review of techniques. Knowl. Eng. Rev. 29 (3), 345–374.
Li, C., 2004. Quantitative distribution of mangroves in Guangxi Zhuang autonomous region. J. Beijing Forestry Univ. 26 (1), 47–52.
Li, W., Guo, Q., Elkan, C., 2010. A positive and unlabeled learning algorithm for one-class classification of remote-sensing data. IEEE Trans. Geosci. Remote Sens. 49 (2), 717–725.
Liang, S., 2000. Characteristics of mangrove communities in Guangxi. Guangxi Sci. 7 (3), 210–216.
Long, J., Napton, D., Giri, C., Graesser, J., 2014. A mapping and monitoring assessment of the Philippines' mangrove forests from 1990 to 2010. J. Coast. Res. 30 (2), 260–271.
Mahdianpari, M., Brisco, B., Granger, J.E., Mohammadimanesh, F., Salehi, B., Banks, S., Weng, Q., 2020. The second generation Canadian wetland inventory map at 10 meters resolution using Google Earth Engine. Can. J. Remote. Sens. 46 (3), 360–375.
Mumby, P.J., Edwards, A.J., Arias-González, J.E., Lindeman, K.C., Blackwell, P.G., Gall, A., Gorczynska, M.I., Harborne, A.R., Pescod, C.L., Renken, H., 2004. Mangroves enhance the biomass of coral reef fish communities in the Caribbean. Nature 427, 533–536.
Muñoz-Marí, J., Bruzzone, L., Camps-Valls, G., 2007. A support vector domain description approach to supervised classification of remote sensing images. IEEE Trans. Geosci. Remote Sens. 45 (8), 2683–2692.
Murphy, S., Hård, J., 2017. Atmospheric Correction of a (Single) Sentinel 2 Image. https://github.com/samsammurphy/gee-atmcorr-S2. (accessed on 3 August 2020).
Nicholls, R.J., Cazenave, A., 2010. Sea-level rise and its impact on coastal zones. Science 328 (5985), 1517–1520.
Olson, D.M., Dinerstein, E., Wikramanayake, E.D., Burgess, N.D., Powell, G.V., Underwood, E.C., Kassem, K.R., 2001. Terrestrial ecoregions of the world: a new map of life on Earth. A new global map of terrestrial ecoregions provides an innovative tool for conserving biodiversity. BioScience 51 (11), 933–938.
Radoux, J., Lamarche, C., Van Bogaert, E., Bontemps, S., Brockmann, C., Defourny, P., 2014. Automated training sample extraction for global land cover mapping. Remote Sens. 6 (5), 3965–3987.
Richards, D.R., Friess, D.A., 2016. Rates and drivers of mangrove deforestation in Southeast Asia, 2000–2012. Proc. Nat. Acad. Sci. 113 (2), 344–349.
Rouse Jr., J.W., Haas, R., Schell, J., Deering, D., 1974. Monitoring Vegetation Systems in the Great Plains with ERTS. Third ERTS Symposium. NASA SP-351, Washington DC, pp. 309–317.
Schaffelke, B., Mellors, J., Duke, N.C., 2005. Water quality in the Great Barrier Reef region: responses of mangrove, seagrass and macroalgal communities. Mar. Pollut. Bull. 51 (1–4), 279–296.
Simard, M., Zhang, K., Rivera-Monroy, V.H., Ross, M.S., Ruiz, P.L., Castañeda-Moya, E., Twilley, R.R., Rodriguez, E., 2006. Mapping height and biomass of mangrove forests in Everglades National Park with SRTM elevation data. Photogramm. Eng. Remote Sens. 299–311, 3.
Spalding, M., Kainuma, M., Collins, L., 2010. World Atlas of Mangroves. Routledge, London, UK.
Tax, D.M., Duin, R.P., 1999a. Data domain description using support vectors. ESANN 99, 251–256.
Tax, D.M., Duin, R.P., 1999b. Support vector domain description. Pattern Recogn. Lett. 20, 1191–1199.
Thomas, N., Lucas, R., Bunting, P., Hardy, A., Rosenqvist, A., Simard, M., 2017. Distribution and drivers of global mangrove forest change, 1996–2010. PLoS One 12 (6), e0179302.
Thomas, N., Bunting, P., Lucas, R., Hardy, A., Rosenqvist, A., Fatoyinbo, T., 2018. Mapping mangrove extent and change: a globally applicable approach. Remote Sens. 10 (9), 1466.
Tian, J., Wang, L., Yin, D., Li, X., Diao, C., Gong, H., Shi, C., Menenti, M., Ge, Y., Nie, S., Ou, Y., Song, X., Liu, X., 2020. Development of spectral-phenological features for deep learning to understand Spartina alterniflora invasion. Remote Sens. Environ. 242, 111745.
Tieng, T., Sharma, S., Mackenzie, R.A., Venkattappa, M., Sasaki, N., Collin, A., 2019. Mapping mangrove forest cover using Landsat-8 imagery, Sentinel-2, very high resolution images and Google Earth Engine algorithm for entire Cambodia. In: IOP Conference Series: Earth and Environmental Science, 266. IOP Publishing, Bristol, UK, p. 012010.
Valiela, I., Bowen, J.L., York, J.K., 2001. Mangrove forests: one of the World's threatened major tropical environments: at least 35% of the area of mangrove forests has been lost in the past two decades, losses that exceed those for tropical rain forests and coral reefs, two other well-known threatened environments. Bioscience 51 (10), 807–815.
Vuolo, F., Żółtak, M., Pipitone, C., Zappa, L., Wenng, H., Immitzer, M., Atzberger, C., 2016. Data service platform for Sentinel-2 surface reflectance and value-added products: system use and examples. Remote Sens. 8 (11), 938.
Wang, L., Diao, C., Xian, G., Yin, D., Lu, Y., Zou, S., Erickson, T.A., 2020. A summary of the special issue on remote sensing of land change science with Google earth engine. Remote Sens. Environ. 248, 112002.
Wang, L., Jia, M., Yin, D., Tian, J., 2019. A review of remote sensing for mangrove forests: 1956–2018. Remote Sens. Environ. 231, 111223.
Wang, X., Xiao, X., Zou, Z., Chen, B., Ma, J., Dong, J., Li, B., 2020. Tracking annual changes of coastal tidal flats in China during 1986–2016 through analyses of Landsat images with Google Earth Engine. Remote Sens. Environ. 238, 110987.
Wilson, R.T., 2013. Py6S: a Python interface to the 6S radiative transfer model. Comput. Geosci. 51, 166–171.
Xu, H., 2006. Modification of normalised difference water index (NDWI) to enhance open water features in remotely sensed imagery. Int. J. Remote Sens. 27 (14), 3025–3033.
Yancho, J.M.M., Jones, T.G., Gandhi, S.R., Ferster, C., Lin, A., Glass, L., 2020. The Google Earth Engine Mangrove Mapping Methodology (GEEMMM). Remote Sens. 12 (22), 3758.
Zhang, Z., Hu, G., Liang, S., 2007. Mangrove resources and conservation in Guangxi. Mar. Environ. Sci. 3.